

*under 3.3*

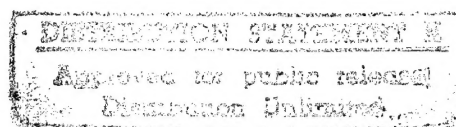
NASA Contractor Report 3088

# Nonlinear Effects on Composite Laminate Thermal Expansion

Z. Hashin, B. W. Rosen, and R. B. Pipes

CONTRACT NAS1-14964  
FEBRUARY 1979

19960207 135



DEPARTMENT OF DEFENSE  
PLASTICS TECHNICAL EVALUATION CENTER  
ARRADCOM, DOVER, N. J. 07801

Status - NTTIS could not supply accession  
the MTR

NASA

DATA RELEASED UNDER E.O. 14176

DATA RELEASED  
E.O. 14176

NASA Contractor Report 3088

# Nonlinear Effects on Composite Laminate Thermal Expansion

Z. Hashin, B. W. Rosen, and R. B. Pipes  
*Materials Sciences Corporation*  
*Blue Bell, Pennsylvania*

Prepared for  
Langley Research Center  
under Contract NAS1-14964



Scientific and Technical  
Information Office

1979

DTIC QUALITY UNRECTED 1

TABLE OF CONTENTS

	<u>Page</u>
LIST OF SYMBOLS. . . . .	v
SUMMARY . . . . .	1
1. INTRODUCTION . . . . .	2
2. THEORY . . . . .	5
2.1 Lamina Thermomechanical Stress-Strain Relations . . . . .	5
2.2 Analysis of Nonlinear Temperature-Dependent Laminates . . . . .	8
2.3 Analysis of $\pm 45^\circ$ Laminate . . . . .	12
3. EXPERIMENTAL PROCEDURE . . . . .	19
Strain Gage Techniques . . . . .	19
Mechanical Characterization of the Lamina. .	21
Thermal Expansion. . . . .	22
Test Procedure for Thermal Expansion Coef- ficients of Loaded $[\pm 45]_5$ Laminates. . . .	24
4. RESULTS AND DISCUSSION . . . . .	25
Properties of Unidirectional Composites . .	25
Properties of $\pm 45^\circ$ Laminates . . . .	25
Free Thermal Expansion . . . . .	26
Influence of Applied Loads. . . . .	29
Discussion . . . . .	30
CONCLUSIONS . . . . .	33
REFERENCES . . . . .	34
TABLES. . . . .	35
FIGURES . . . . .	46

### LIST OF SYMBOLS

A	- Fiber direction;
$\underline{C}$	- stiffness matrix of lamina;
$\underline{C}^{(k)}$	- stiffness matrix referred to lamina material coordinates;
$(k) \underline{C}$	- stiffness matrix referred to laminate coordinates;
$\underline{C}^*$	- effective stiffness matrix of laminate;
E	- Young's modulus;
$E_A$	- Young's modulus in fiber direction;
$E_T$	- Young's modulus transverse to fibers;
$G_A$	- inplane shear modulus of lamina;
h	- half thickness of laminate;
k	- lamina index;
m	- exponent in Ramberg-Osgood stress-strain relation;
n	- exponent in Ramberg-Osgood stress-strain relation;
$s_g$	- gage factor;
$t_k$	- thickness of lamina;
$\underline{T}^{(k)}$	- transformation matrix of kth lamina;
$x_1^{(k)}, x_2^{(k)}$	- material coordinates of kth lamina;
$(k) x_1, (k) x_2$	- laminate coordinates of kth lamina;
$\alpha, \beta$	- subscripts ranging over 1,2;

LIST OF SYMBOLS (Continued)

- $\alpha_A$  - longitudinal thermal expansion coefficient of lamina;
- $\alpha_T$  - transverse thermal expansion coefficient of lamina;
- $\underline{\alpha}^{(k)}$  - thermal expansion matrix of lamina in material axes;
- $\underline{\alpha}^{(k)}$  - thermal expansion matrix of lamina in laminate axes;
- $\underline{\alpha}^*$  - effective thermal expansion matrix of loaded laminate;
- $\alpha_1^*, \alpha_2^*$  - effective thermal expansion coefficients of  $\pm 45^\circ$  laminate in load and transverse to load directions;
- $\underline{\alpha}_f^*$  - free thermal expansion matrix of laminate;
- $\alpha_g$  - thermal expansion coefficient of grid (gage);
- $\alpha_p$  - thermal expansion coefficient of polyimide;
- $\alpha_q$  - thermal expansion coefficient of quartz;
- $\alpha_s$  - thermal expansion coefficient of substrate;
- $\gamma$  - gage coefficient of resistivity;
- $\underline{\Gamma}^*$  - effective thermomechanical stiffness matrix of laminate;
- $\epsilon$  - strain;
- $\underline{\epsilon}^{(k)}$  - lamina strain in material axes;
- $\underline{\epsilon}^{(k)}$  - lamina strain in laminate axes;
- $\overset{\circ}{\underline{\epsilon}}$  - laminate uniform strain;
- $\epsilon'_{\alpha\beta}$  - linear strain

LIST OF SYMBOLS (Concluded)

$\epsilon_{\alpha\beta}''$	- nonlinear strain;
$\epsilon_{\alpha\beta}^\phi$	- free thermal strain;
$\epsilon_{app}$	- apparent strain;
$\epsilon_p$	- strain in polyimide;
$\epsilon_q$	- strain in quartz;
$\sigma$	- stress;
$\underline{\sigma}^{(k)}$	- lamina stress in material axes;
$^{(k)}\underline{\sigma}$	- lamina stress in laminate axes;
$\overset{\circ}{\underline{\sigma}}$	- applied laminate edge stress;
$\sigma_{\alpha\beta}$	- plane stress;
$\overline{\sigma}_y$	- transverse lamina stress parameter;
$\tau_y$	- inplane lamina shear stress parameter;
$\theta_k$	- angle of reinforcement of lamina;
$\phi$	- temperature;
$\phi_0$	- stress-free temperature;
$\Delta_\phi$	- temperature increment.

### SUMMARY

The thermomechanical behavior of unidirectionally fiber reinforced laminae in plane stress has been described by a set of nonlinear thermomechanical stress-strain relations. A general procedure for analysis of in-plane loaded symmetric laminates, composed of such laminae, has been established for simultaneous loading and temperature inputs. A  $\pm 45^\circ$  laminate subjected to heating and uniaxial load has been analyzed in detail.

Analyses of Graphite/Polyimide laminates have shown that the thermomechanical strains cannot be separated into mechanical strain and free thermal expansion strain. Consequently the free thermal expansion coefficient is generally not useful for computation of thermal strains in a loaded nonlinear laminate. Moreover, a laminate such as the  $\pm 45^\circ$  which behaves isotropically for free thermal expansion behaves anisotropically when loaded and heated.

Elastic properties and thermal expansion coefficients of unidirectional Graphite/Polyimide specimens were measured as a function of temperature to provide inputs for the analysis. The  $\pm 45^\circ$  symmetric Graphite/Polyimide laminates were tested to obtain free thermal expansion coefficients and thermal expansion coefficients under various uniaxial loads.

The experimental results demonstrated the effects predicted by the analysis, namely dependence of thermal expansion coefficients on load, and anisotropy of thermal expansion under load. Numerical agreement of analytical and experimental results was fair. The significance of time dependence on thermal expansion was demonstrated by comparison of measured laminate free expansion coefficients with and without 15-day delay at intermediate temperature.

## 1. INTRODUCTION

Determination of the thermoelastic properties of fiber composite laminates on the basis of the thermoelastic properties of the constituting laminae and their stacking sequence is a routine procedure used by composite materials analysts. Even when the thermoelastic properties of the laminae are temperature dependent, the determination of laminate properties is of conventional nature, provided the laminae are elastic at all temperatures.

In recent years, nonlinear mechanical properties of laminates have been successfully incorporated into laminate analysis, primarily in the isothermal case. In the case of Boron/epoxy and Graphite/epoxy layers, room-temperature nonlinearity is exhibited primarily in shear and transverse tension and compression. Room-temperature laminate stiffness properties are affected by this nonlinearity, but not drastically. The most significant nonlinearities are exhibited by the  $\pm 45^\circ$  laminate under uniaxial loading.

The situation appears to be significantly different in the case of laminates subjected to large temperature changes. This is due to two phenomena. The first is that nonlinear behavior of a unidirectional lamina results from matrix nonlinearity which increases significantly with temperature. The second is that large thermal expansion coefficients exist in directions normal to the fibers of a unidirectional laminae. Therefore, as a result of temperature changes, large transverse stresses or strains will be induced even for a fiber-dominated laminate. It is to be expected that nonlinearity in the fiber direction can be neglected since the fibers remain stiff and elastic. However, nonlinear effects of the stress-strain relation in a direction transverse to the fibers, and in shear, both increase with temperature and have to be considered. Moreover, these transverse and shear effects are not superposable, but are interactive; i.e. the nonlinear shear strain depends also on the transverse strain

and vice versa. These nonlinearities may have a very significant effect upon thermal expansion coefficients even when the effect upon laminate stiffnesses is small.

In addition, epoxies and polyimides exhibit time-dependent effects whose significance also increases with temperature. Therefore, internal stresses and strains change even when temperatures and loads are held constant. In the first approximation, such behavior can be modeled as viscoelastic.

The above effects can be expected to occur to some extent in laminates designed for moderately elevated temperature applications. The possible consequences of these effects include the following:

- 1) laminate thermal expansion coefficients and internal stresses as determined by conventional thermoelastic analysis will be incorrect;
- 2) laminate thermal expansion coefficients and internal stresses will be time dependent; and
- 3) the deformations and stresses of a laminate subjected to loads and temperature changes will not be correctly obtained by adding stresses and strains due to loads alone to those obtained due to temperature changes alone.

The temperature-dependence problem has been reported, e.g. in references [1] and [2]. The general approach is that one takes as a starting point the stress-free temperature. (It is important to emphasize that depending upon the fabrication process, this may actually mean a temperature different from room temperature at which all stresses in the laminate vanish.) One may then imagine an experiment in which free thermal expansion of each layer takes place from the stress-free temperature to the final temperature or temperature distribution. At the final temperature, one may then apply stresses to satisfy equilibrium and compatibility and reassemble the laminate. Hence, it follows that the final stress

distribution is obtained by using secant  $\Delta L/L$  values from the stress-free temperature to the final temperature and by using elastic constants at the final temperature. The incremental theory has been shown in reference [2] to be obtainable from the total strain theory outlined above.

Time-dependent properties have been treated by a number of authors, and methods of varying complexity exist in the literature (e.g. refs. [3] to [6]). Similarly, for stress-dependent phenomena in isothermal laminate analysis, there is a significant body of literature (e.g. refs. [7] to [11]). For both of these problems, the various existing analytical methods have various limitations.

In the present work there is established a general procedure to compute the thermomechanical properties and internal stresses of laminates composed of nonlinear temperature dependent laminae. The methods used are similar to those employed in reference [7] for isothermal nonlinear laminates.

In addition to the analytical investigation an experimental program has been carried out whose purpose is to measure thermal expansion coefficients of free and loaded Graphite/Polyimide laminae in order to examine the validity of the analytical results.

## 2. THEORY

### 2.1 Lamina Thermomechanical Stress-Strain Relations

The approach to be adopted is a generalization of the method of reference [7] for isothermal nonlinear stress-strain relations for plane stress.

The lamina state of stress is  $\sigma_{11}$ ,  $\sigma_{22}$ ,  $\sigma_{12}$ , where  $x_1$  is in the fiber direction and  $x_2$  is in the transverse direction (fig. 1).

The strains in the lamina plane are given by:

$$\epsilon_{\alpha\beta} = \epsilon'_{\alpha\beta} + \epsilon''_{\alpha\beta} + \epsilon^\phi_{\alpha\beta} \quad (2.1.1)$$

where  $\epsilon'_{\alpha\beta}$  is the linear elastic strain,  $\epsilon''_{\alpha\beta}$  is the nonlinear part of the strain,  $\epsilon^\phi_{\alpha\beta}$  is the free thermal strain, and Greek indices such as  $\alpha$  and  $\beta$  range over 1,2.

The strains  $\epsilon'_{\alpha\beta}$  have the form:

$$\begin{aligned} \epsilon'_{11} &= s'_{11}(\phi) \sigma_{11} + s'_{12}(\phi) \sigma_{22} \\ \epsilon'_{22} &= s'_{12}(\phi) \sigma_{11} + s'_{22}(\phi) \sigma_{22} \\ \epsilon'_{12} &= 2s'_{66}(\phi) \sigma_{12} \end{aligned} \quad (2.1.2)$$

where  $\phi$  is the temperature.

The compliances in (2.1.2) can also be written in the form:

$$s'_{11} = \frac{1}{E_A(\phi)}$$

$$s'_{12} = -\frac{v_A(\phi)}{E_A(\phi)}$$

$$s'_{22} = \frac{1}{E_T(\phi)}$$

$$s'_{66} = \frac{1}{4G_A(\phi)}$$

where  $E_A$ ,  $\nu_A$ ,  $E_T$ ,  $G_A$  are temperature dependent axial Young's modulus, axial Poisson's ratio, transverse Young's modulus, and axial shear modulus, respectively.

It is assumed that because of large fiber stiffness, the nonlinear strain  $\epsilon''_{11}$  vanishes and that  $\sigma_{11}$  has no effect on the strains  $\epsilon''_{22}$  and  $\epsilon''_{12}$ . Consequently, the nonlinear strains can be written as:

$$\epsilon''_{11} = 0$$

$$\epsilon''_{22} = s''_{22} (\sigma_{22}, \sigma_{12}, \phi) \sigma_{22} \quad (2.1.4)$$

$$\epsilon''_{12} = 2s''_{66} (\sigma_{22}, \sigma_{12}, \phi) \sigma_{12}$$

where  $s''_{22}$  and  $s''_{66}$  are nonlinear temperature dependent (secant) compliances.

The one-dimensional isothermal responses to  $\sigma_{22}$  and to  $\sigma_{12}$ , each of them acting separately, are modeled in the familiar Ramberg-Osgood form:

$$\epsilon''_{22} = \epsilon'_{22} + \epsilon''_{22} = \frac{\sigma_{22}}{E_T} \left[ 1 + \left( \frac{\sigma_{22}}{\sigma_y} \right)^{m-1} \right] \quad (2.1.5)$$

$$\epsilon''_{12} = \epsilon'_{12} + \epsilon''_{12} = \frac{\sigma_{12}}{2G_A} \left[ 1 + \left( \frac{\sigma_{12}}{\tau_y} \right)^{n-1} \right]$$

where  $\sigma_y$  and  $\tau_y$  are temperature dependent stress parameters and  $m$  and  $n$  are exponents which may also be temperature dependent. These four quantities are to be regarded as curve fitting parameters to best fit the experimental data.

Employing the same reasoning as in [7], it follows that in the case of combined stresses  $\sigma_{\alpha\beta}$ , the nonlinear parts of the strains are given by:

$$\epsilon_{22}'' = \frac{\sigma_{22}}{E_T} \left[ \left( \frac{\sigma_{22}}{\sigma_Y} \right)^2 + \left( \frac{\sigma_{12}}{\tau_Y} \right)^2 \right] \frac{m-1}{2} \quad (2.1.6)$$

$$\epsilon_{12}'' = \frac{\sigma_{12}}{2G_A} \left[ \left( \frac{\sigma_{22}}{\sigma_Y} \right)^2 + \left( \frac{\sigma_{12}}{\tau_Y} \right)^2 \right] \frac{n-1}{2}$$

Finally, the free thermal strains  $\epsilon_{\alpha\beta}^\phi$  in (2.1.1) are written in the form:

$$\begin{aligned} \epsilon_{11}^\phi &= \alpha_A(\phi) \phi \\ \epsilon_{22}^\phi &= \alpha_T(\phi) \phi \end{aligned} \quad (2.1.7)$$

where  $\alpha_A$  and  $\alpha_T$  are axial and transverse temperature-dependent (secant) thermal expansion coefficients assumed to be stress independent.

Summarizing equations (2.1.1) through (2.1.7), we have the following nonlinear temperature dependent stress-strain relations:

$$\begin{aligned} \epsilon_{11} &= \frac{1}{E_A(\phi)} \sigma_{11} - \frac{\nu_A(\phi)}{E_A(\phi)} \sigma_{22} + \alpha_A(\phi) \phi \\ \epsilon_{22} &= \frac{\nu_A(\phi)}{E_A(\phi)} \sigma_{11} + \frac{1}{E_T(\phi)} \left\{ 1 + \left[ \left( \frac{\sigma_{22}}{\sigma_Y(\phi)} \right)^2 + \left( \frac{\sigma_{12}}{\tau_Y(\phi)} \right)^2 \right] \frac{m-1}{2} \right\} \sigma_{22} \\ &\quad + \alpha_T(\phi) \phi \\ \epsilon_{12} &= \frac{1}{2G_A(\phi)} \left\{ 1 + \left[ \left( \frac{\sigma_{22}}{\sigma_Y(\phi)} \right)^2 + \left( \frac{\sigma_{12}}{\tau_Y(\phi)} \right)^2 \right] \frac{n-1}{2} \right\} \sigma_{12} \end{aligned} \quad (2.1.8)$$

## 2.2 Analysis of Nonlinear Temperature Dependent Laminates

Consider a balanced symmetric laminate loaded on its edges by uniformly distributed stresses and subjected to the temperature rise  $\phi$ .

The following problems are to be considered: (i) find the stresses in the laminae; (ii) find the effective thermo-mechanical stress-strain relations of the laminate.

The laminate is referred to a fixed system of coordinates  $x_1, x_2$  (fig. 1). Any lamina,  $k$ th say, is referred to its material system of coordinates,  $x_1^{(k)}$  in fiber direction and  $x_2^{(k)}$  transverse to fiber direction (fig. 2). The fiber orientation of the  $k$ th lamina is defined by the angle:

$$\theta_k = \hat{x} x_1, x_1^{(k)} = \hat{x} x_2, x_2^{(k)} \quad (2.2.1)$$

The stress-strain relation of the lamina in its material system is:

$$\underline{\varepsilon}^{(k)} = \underline{S} \underline{\sigma}^{(k)} + \underline{\alpha} \phi \quad (2.2.2)$$

where underbars denote tensors. Here  $\underline{S}$  is the temperature and stress dependent compliance tensor and  $\underline{\alpha}$  the temperature dependent thermal expansion tensor as defined by (2.1.8).

It may be easily shown by trivial considerations of heat conduction theory that the temperature throughout all laminae is the same constant  $\phi$ . Also in accordance with usual laminate theory: (i) all laminae are in states of plane stress; (ii) the strains in all laminae as referred to the laminate fixed coordinate system  $x_1, x_2$  are the same uniform  $\varepsilon_{\alpha\beta}$ .

These considerations make it possible to construct a set of nonlinear equations for computation of all laminae stresses.

First, define the transformation tensor  $T^{(k)}$  by:

$$^{(k)} \underline{\sigma} = \underline{T}^{(k)} \underline{\sigma}^{(k)} \quad (2.2.3)$$

where  $\sigma^{(k)}$  is the lamina stress referred to the material system and  $\sigma^{(k)}$  is the same stress referred to the laminate system.

The matrix of  $T^{(k)}$  is given by:

$$[\underline{T}^{(k)}] = \begin{bmatrix} \cos^2 \theta_k & \sin^2 \theta_k & -2\cos \theta_k \sin \theta_k \\ \sin^2 \theta_k & \cos^2 \theta_k & 2\cos \theta_k \sin \theta_k \\ \sin \theta_k \cos \theta_k & -\sin \theta_k \cos \theta_k & \cos^2 \theta_k - \sin^2 \theta_k \end{bmatrix} \quad (2.2.4)$$

Similarly,

$$(\underline{\sigma}) \underline{\varepsilon} = \underline{T}^k \underline{\varepsilon}^{(k)} \quad (2.2.5)$$

It follows from equilibrium that

$$\sum_{k=1}^K (\underline{\sigma}) \underline{\sigma} t_k = \underline{\sigma}^0 h \quad (2.2.6)$$

where:

2K - number of laminae;

2h - thickness of laminate;

$t_k$  - thickness of kth lamina;

and  $\underline{\sigma}$  has components  $\sigma_{\alpha\beta}^0$ , i.e. the stresses  $\sigma_{11}^0$ ,  $\sigma_{22}^0$ , and  $\sigma_{12}^0$  applied to the laminate edges.

By hypothesis (b)

$$(1) \underline{\varepsilon} = (2) \underline{\varepsilon} = \dots = (k) \underline{\varepsilon} = (K) \underline{\varepsilon} \quad (2.2.7)$$

Now introduce (2.2.3) into (2.2.6), (2.2.2) into (2.2.5) and subsequently into (2.2.7). The results are:

$$\sum_{k=1}^K \underline{T}^{(k)} \underline{\sigma}^{(k)} t_k = \underline{\sigma}^0 h \quad (2.2.8)$$

$$\underline{T}^{(1)} \underline{S} \underline{\sigma}^{(1)} + \underline{T}^{(1)} \underline{\alpha\phi} = \underline{T}^{(2)} \underline{S} \underline{\sigma}^{(2)} + \underline{T}^{(2)} \underline{\alpha\phi} = \dots$$

$$\begin{aligned} \underline{T}^{(k)} \underline{S} \underline{\sigma}^{(k)} + \underline{T}^{(k)} \underline{\alpha\phi} = \\ \underline{T}^{(K)} \underline{S} \underline{\sigma}^{(K)} + \underline{T}^{(K)} \underline{\alpha\phi} \end{aligned} \quad (2.2.9)$$

Since  $\underline{\sigma}^0$  has three components, there are altogether  $3K$  unknown laminae stresses. To determine these we have the three equations (2.2.8) and the  $3(K-1)$  equations (2.2.9), in all  $3K$  nonlinear equations.

Once the laminae stresses are known, the effective thermomechanical stress-strain relations of the laminate can be determined in the following fashion. Write (2.2.2) in the laminate coordinate system:

$$(k) \underline{\varepsilon} = (k) \underline{S} \underline{\sigma}^{(k)} + (k) \underline{\alpha\phi} \quad (2.2.10)$$

All tensors in (2.2.10) are obtained from their counterparts in (2.2.2) by the transformation (2.2.3).

Define:

$$(k) \underline{C} = (k) \underline{S}^{-1} \quad (2.2.11)$$

where the inversion has to be carried out for  $(k) \underline{S}$  components computed as functions of the lamina stresses. Since also by (2.2.7)  $(k) \underline{\varepsilon}$  is the laminate uniform strain  $\underline{\varepsilon}^0$ , (2.2.10) can be written as:

$$(k) \underline{\sigma} = (k) \underline{C} \underline{\varepsilon}^0 - (k) \underline{C} (k) \underline{\alpha\phi} \quad (2.2.12)$$

Substituting (2.2.12) into (2.2.8) gives:

$$\overset{\circ}{\underline{\sigma}} = \underline{C}^* \overset{\circ}{\underline{\epsilon}} + \underline{\Gamma}^* \phi \quad (2.2.13)$$

where

$$\underline{C}^* = \sum_{k=1}^K \overset{(k)}{\underline{C}} \underline{t}_k / h \quad (a)$$

$$\underline{\Gamma}^* = - \sum_{k=1}^K \overset{(k)}{\underline{C}} \underline{\alpha} \underline{t}_k / h \quad (b) \quad (2.2.14)$$

Equation (2.2.13) formally resembles an effective thermo-elastic stress-strain relation. It is nonlinear since  $\underline{C}^*$  and  $\underline{\Gamma}^*$  depend on the laminae stresses.

The inversion of (2.2.13) is:

$$\overset{\circ}{\underline{\epsilon}} = \underline{S}^* \overset{\circ}{\underline{\sigma}} + \underline{\alpha}^* \phi \quad (2.2.15)$$

where

$$\underline{S}^* = (\underline{C}^*)^{-1} = \underline{S}^*(\overset{\circ}{\underline{\sigma}}, \phi) \quad (a)$$

$$\underline{\alpha}^* = -\underline{S}^* \underline{\Gamma}^* = \underline{\alpha}^*(\overset{\circ}{\underline{\sigma}}, \phi) \quad (b) \quad (2.2.16)$$

It is seen that (2.2.16a) are the nonlinear compliances of the laminate while (2.2.16b) are its nonlinear stress dependent thermal expansion coefficients.

The usual definition of thermal expansion coefficients is based on heating of an unloaded body. If this is done in the present case, equations (2.2.6) - (2.2.8) become:

$$\sum_{k=1}^K \overset{(k)}{\underline{\sigma}} \underline{t}_k = \sum_{k=1}^K \overset{(k)}{\underline{T}} \overset{(k)}{\underline{\sigma}} \underline{t}_k = 0 \quad (2.2.17)$$

The last of (2.2.17) together with (2.2.9) now determine the laminae stresses.

Repeating the same procedure as previously used it follows that:

$$\underline{\varepsilon} = \underline{\alpha}^* \phi \quad (2.2.18)$$

where  $\underline{\alpha}^*$  is defined by (2.2.16b), (2.2.14b) and (2.2.11).

Note, however, that since the laminae stresses in the present free body heating problem will be different from the previous ones, the thermal expansion coefficients defined by (2.2.18) are in general different from the ones obtained in the case of laminate loading and heating. Indeed, the thermal expansion coefficient in (2.2.18) can be written as a special case of (2.2.16b); i.e.:

$$\underline{\alpha}^* = \alpha^*(0, \phi) \quad (2.2.19)$$

Consequently, the classical concept of thermal expansion coefficient is not useful in the case of a nonlinear laminate since the strains due to loading and heating can no longer be found by super-position of mechanical and thermal strains. Instead, the laminate strains must be found on the basis of the interactive effect of loading and heating.

### 2.3 Analysis of $\pm 45^\circ$ Laminate

The general analysis of paragraph 2.2 will now be applied to the case of a balanced  $\pm 45^\circ$  laminate which is heated and subjected to uniaxial stress (fig. 3). From symmetry considerations:

$$\begin{array}{lll} \sigma_{11}^1 = \sigma_{11}^2 & \sigma_{22}^1 = \sigma_{22}^2 & \sigma_{12}^1 = -\sigma_{12}^2 \\ 1_{\sigma_{11}} = 2_{\sigma_{11}} & 1_{\sigma_{22}} = 2_{\sigma_{22}} & 1_{\sigma_{12}} = -2_{\sigma_{12}} \end{array} \quad (2.3.1)$$

The stress transformation (2.2.3-4) with  $\theta = 45^\circ$  yields:

$$\begin{aligned} {}^1\sigma_{11} &= \frac{1}{2} \sigma_{11}^1 + \frac{1}{2} \sigma_{22}^1 - \sigma_{12}^1 \\ {}^1\sigma_{22} &= \frac{1}{2} \sigma_{11}^1 + \frac{1}{2} \sigma_{22}^1 + \sigma_{12}^1 \\ {}^1\sigma_{12} &= \frac{1}{2} \sigma_{11}^1 - \frac{1}{2} \sigma_{22}^1 \end{aligned} \quad (2.3.2)$$

The three equations of equilibrium (2.2.6) assume the form:

$$\begin{aligned} {}^1\sigma_{11} + {}^2\sigma_{11} &= {}^2\sigma_{11} \\ {}^1\sigma_{22} + {}^2\sigma_{22} &= 0 \\ {}^1\sigma_{12} + {}^2\sigma_{12} &= 0 \end{aligned} \quad (2.3.3)$$

In view of (2.3.1) and (2.3.2), equations (2.2.3) become:

$$\begin{aligned} \sigma_{11}^1 + \sigma_{22}^1 - 2\sigma_{12}^1 &= {}^2\sigma_{11} \\ \sigma_{11}^1 + \sigma_{22}^1 + 2\sigma_{12}^1 &= 0 \end{aligned} \quad (2.3.4)$$

the last of equation (2.3.3) is identically satisfied.

Adding and subtracting equations (2.3.4) gives:

$$\begin{aligned} \sigma_{11}^1 + \sigma_{22}^1 + {}^2\sigma_{11} &\quad (a) \\ \sigma_{12}^1 &= -\frac{1}{2} {}^2\sigma_{11} \quad (b) \end{aligned} \quad (2.3.5)$$

thus determining the lamina shear stress.

The lamina strains are given by:

$$\begin{aligned}\epsilon_{11}^1 + s_{11}\sigma_{11}^1 + s_{12}\sigma_{22}^1 + \alpha_1\phi \\ \epsilon_{22}^1 + s_{12}\sigma_{11}^1 + s_{22}\sigma_{22}^1 + \alpha_2\phi \\ \epsilon_{12}^1 = \sigma_{12}^1/2G\end{aligned}\quad (2.3.6)$$

where according to (2.1.8):

$$\begin{aligned}s_{11} &= \frac{1}{E_A(\phi)} \\ s_{12} &= \frac{-v_A(\phi)}{E_A(\phi)} \\ s_{22} &= \frac{1}{E_T(\phi)} \left\{ 1 + \left[ \left( \frac{\sigma_{22}^1}{\sigma_Y(\phi)} \right)^2 + \left( \frac{\sigma_{12}^1}{\tau_Y(\phi)} \right)^2 \right] \frac{m-1}{2} \right\} \\ \frac{1}{G} &= \frac{1}{G_A(\phi)} \left\{ 1 + \left[ \left( \frac{\sigma_{22}^1}{\sigma_Y(\phi)} \right)^2 + \left( \frac{\sigma_{12}^1}{\tau_Y(\phi)} \right)^2 \right] \frac{n-1}{2} \right\} \\ \alpha_1 &= \alpha_A(\phi) \\ \alpha_2 &= \alpha_T(\phi)\end{aligned}\quad (2.3.7)$$

From symmetry

$$\epsilon_{12}^1 + \epsilon_{21}^1 = 0 \quad (2.3.8)$$

Therefore:

$$\epsilon_{11}^1 = \epsilon_{22}^1 \quad (2.3.9)$$

Introducing (2.3.6) into (2.3.9) gives:

$$(s_{11} - s_{12}) \sigma_{11}^1 + (s_{12} - s_{22}) \sigma_{22}^1 = (\alpha_2 - \alpha_1) \phi \quad (2.3.10)$$

Equation (2.3.10) contains the stresses  $\sigma_{22}^1$  and  $\sigma_{12}^1$  in non-linear form. Together with (2.3.5) it determines the stresses  $\sigma_{11}^1$  and  $\sigma_{22}^1$ . Eliminating  $\sigma_{11}^1$  between these two equations and using (2.3.5b) yields the result:

$$\sigma_{22}^1 \left\{ 1 + 2\nu_A + \frac{E_A}{E_T} \left[ 1 + \left[ \left( \frac{\sigma_{22}^1}{\sigma_Y} \right)^2 + \left( \frac{\sigma_{11}^1}{\sigma_Y} \right)^2 \right]^{\frac{m-1}{2}} \right] \right\} - (1 + \nu_A) \sigma_{11}^1 + E_A (\alpha_T - \alpha_A) \phi = 0 \quad (2.3.11)$$

which determines  $\sigma_{22}^1$ .

The laminate normal strains are given in terms of tensor transformation and use of (2.3.9) by:

$$\begin{aligned} {}^0 \varepsilon_{11} &= {}^1 \varepsilon_{11} = \varepsilon_{11}^1 - \varepsilon_{12}^1 \\ {}^0 \varepsilon_{22} &= {}^1 \varepsilon_{22} = \varepsilon_{11}^1 + \varepsilon_{12}^1 \end{aligned} \quad (2.3.12)$$

From (2.3.7), (2.3.6), (2.3.5a) and (2.3.12):

$$\begin{aligned} {}^0 \varepsilon_{11} ({}^0 \sigma_{11}, \phi) &= \frac{{}^0 \sigma_{11}}{E_A} - \frac{1+\nu_A}{E_A} \sigma_{22}^1 + \\ \frac{{}^0 \sigma_{11}}{4G_A} &\left\{ 1 + \left[ \left( \frac{\sigma_{22}^1}{\sigma_Y} \right)^2 + \left( \frac{{}^0 \sigma_{11}}{2\tau_Y} \right)^2 \right]^{\frac{n-1}{2}} \right\} + \alpha_A \phi \end{aligned}$$

$$\begin{aligned} \overset{\circ}{\epsilon}_{22}(\overset{\circ}{\sigma}_{11}, \phi) &= \frac{\overset{\circ}{\sigma}_{11}}{E_A} - \frac{1+\nu_A}{E_A} \overset{\circ}{\sigma}_{22}^1 - \\ &\frac{\overset{\circ}{\sigma}_{11}}{4G_A} \left\{ 1 + \left[ \left( \frac{\overset{\circ}{\sigma}_{22}^1}{\sigma_Y} \right)^2 + \left( \frac{\overset{\circ}{\sigma}_{11}}{2\tau_Y} \right)^2 \right]^{\frac{m-1}{2}} \right\} + \alpha_A \phi \end{aligned} \quad (2.3.13)$$

Next some special cases are considered: Let the laminate first be heated without loading. Then (2.3.11) becomes:

$$\overset{\circ}{\sigma}_{22}^1 \left\{ 1 + 2\nu_A + \frac{E_A}{E_T} \left[ 1 + \left( \frac{\overset{\circ}{\sigma}_{22}^1}{\sigma_Y} \right)^{m-1} \right] \right\} + E_A (\alpha_T - \alpha_A) \phi = 0 \quad (2.3.14)$$

The laminate strains are then from (2.3.13):

$$\overset{\circ}{\epsilon}_{11}(0, \phi) = \overset{\circ}{\epsilon}_{22}(0, \phi) = - \frac{1+\nu_A}{E_A} \overset{\circ}{\sigma}_{22}^1 + \alpha_A \phi \quad (2.3.15)$$

where  $\overset{\circ}{\sigma}_{22}^1$  in (2.3.15) is defined by (2.3.14). Consequently, the free thermal expansion coefficient  $\alpha_f^*$  of the laminate is given by:

$$\alpha_f^* = - \frac{1+\nu_A}{\phi E_A} \overset{\circ}{\sigma}_{22}^1 + \alpha_A \quad (2.3.16)$$

Now let the laminate be subjected to the axial stress  $\overset{\circ}{\sigma}_{11}$  with  $\phi=0$ . Then  $\overset{\circ}{\sigma}_{22}^1$  is defined from (2.3.11) by:

$$\begin{aligned} \overset{\circ}{\sigma}_{22}^1 \left\{ 1 + 2\nu_A + \frac{E_A}{E_T} \left[ 1 + \left[ \left( \frac{\overset{\circ}{\sigma}_{22}^1}{\sigma_Y} \right)^2 + \left( \frac{\overset{\circ}{\sigma}_{11}}{2\tau_Y} \right)^2 \right]^{\frac{m-1}{2}} \right] \right\} - \\ (1 + \nu_A) \overset{\circ}{\sigma}_{11} = 0 \end{aligned} \quad (2.3.17)$$

and the strains are:

$$\begin{aligned}
{}^{\circ}\varepsilon_{11}({}^{\circ}\sigma_{11}, 0) &= \frac{{}^{\circ}\sigma_{11}}{E_A} - \frac{1+\nu_A}{E_A} \sigma_{22}^1 + \\
&\quad \frac{{}^{\circ}\sigma_{11}}{4G_A} \left\{ 1 + \left[ \left( \frac{\sigma_{22}^1}{\sigma_y} \right)^2 + \left( \frac{{}^{\circ}\sigma_{11}}{2\tau_y} \right)^2 \right] \frac{n-1}{2} \right\} \\
{}^{\circ}\varepsilon_{22}({}^{\circ}\sigma_{11}, 0) &= \frac{{}^{\circ}\sigma_{11}}{E_A} - \frac{1+\nu_A}{E_A} \sigma_{22}^1 - \\
&\quad \frac{{}^{\circ}\sigma_{11}}{4G_A} \left\{ 1 + \left[ \left( \frac{\sigma_{22}^1}{\sigma_y} \right)^2 + \left( \frac{{}^{\circ}\sigma_{11}}{2\tau_y} \right)^2 \right] \frac{n-1}{2} \right\} \tag{2.3.18}
\end{aligned}$$

By conventional definition the expansion coefficients are given by:

$$\begin{aligned}
\alpha_1^* &= \frac{1}{\phi} {}^{\circ}\varepsilon_{11}({}^{\circ}\sigma_{11}, \phi) - {}^{\circ}\varepsilon_{11}({}^{\circ}\sigma_{11}, 0) \\
\alpha_2^* &= \frac{1}{\phi} {}^{\circ}\varepsilon_{22}({}^{\circ}\sigma_{11}, \phi) - {}^{\circ}\varepsilon_{22}({}^{\circ}\sigma_{11}, 0) \tag{2.3.19}
\end{aligned}$$

It is seen that the expansion coefficients as defined by (2.3.19) are load dependent, different from the free expansion coefficients (2.3.16) and in fact unequal. Thus the thermal expansion of the laminate has become anisotropic due to load application.

Conventional linear thermoelastic analysis is contained in the preceding results as a special case when:

$$\sigma_y \gg \sigma_{22}^1$$

$$\tau_y \gg \sigma_{12}^1$$

which implies that nonlinear effects are negligible. In this case we have for free thermal expansion from (2.3.14) and

(2.3.16) :

$$\sigma_{22}^1 = \frac{E_A (\alpha_A - \alpha_T) \phi}{1 + 2\nu_A + E_A/E_T}$$
$$\alpha_f^* = \alpha_A + \frac{(\alpha_T - \alpha_A) (1 + \nu_A)}{1 + 2\nu_A + E_A/E_T} \quad (2.3.20)$$

which are the well-known thermoelastic results.

It also follows from (2.3.11) and (2.3.13) that for heating and loading:

$$\epsilon_{11}^0 (\sigma_{11}^0, \phi) = \frac{\sigma_{11}^0}{E_1^*} + \alpha_f^* \phi \quad (2.3.21)$$
$$\epsilon_{22}^0 (\sigma_{11}^0, \phi) = - \frac{\nu_{12}^*}{E_1^*} \sigma_{11}^0 + \alpha_f^* \phi$$

where  $E_1^*$  and  $\nu_{12}^*$  are the laminate Young's modulus and associated Poisson's ratio at temperature  $\phi$ .

### 3. EXPERIMENTAL PROCEDURE

#### Strain Gage Techniques

For the constant temperature mechanical tests the quarter bridge strain gage circuit was used since no temperature compensation was needed. A temperature compensated half wheatstone bridge circuit was used for measuring the material thermal response over the  $-53^{\circ}\text{C}$  to  $260^{\circ}\text{C}$  ( $-65^{\circ}\text{F}$  to  $+500^{\circ}\text{F}$ ) temperature range to eliminate the nonlinear effects from the changes in resistivity of the gage.

In the half bridge circuit (fig. 4) the active gage was bonded to the test specimen and the compensating gage bonded to the quartz standard with a known coefficient of thermal expansion (Dynasil Corp.,  $\alpha = 1.82\mu\text{e}/^{\circ}\text{C}$ ). The resulting strain output from this circuit is the difference between the active and compensating gage. Knowing that the relationship between the apparent strain and the thermal coefficients of the gage and substrate is:

$$\alpha_s = \alpha_g + \epsilon_{app}/\Delta\phi - \gamma S_g,$$

where;

$\alpha_s$  = coefficient of thermal expansion of substrate;

$\alpha_g$  = coefficient of thermal expansion of grid (gage);

$\epsilon_{app}$  = apparent strain;

$\gamma$  = coefficient of resistivity of gage;

$S_g$  = gage factor.

For a given temperature excursion  $\Delta\phi$ :

$$\alpha_p = \alpha_g + \epsilon_p/\Delta\phi - \gamma/S_g; \quad (3.1)$$

$$\alpha_q = \alpha_g + \epsilon_q/\Delta\phi - \gamma/S_g; \quad (3.2)$$

where subscripts p and q refer to the Graphite/Polyimide substrate and quartz, respectively.

Subtracting and assuming identical gages on each material:

$$\alpha_p - \alpha_q = \frac{\epsilon_p - \epsilon_q}{\Delta\phi}$$

where the resistivity and  $\alpha$  grid are eliminated. The apparent strain difference  $(\epsilon_p - \epsilon_q)$  is measured in the half bridge circuit. Therefore, the thermal coefficient of expansion for the polyimide is:

$$\alpha_p = (\epsilon_p - \epsilon_q)/\Delta\phi + \alpha_q. \quad (3.3)$$

Where  $(\epsilon_p - \epsilon_q)/\Delta\phi$  is easily found from the slope of the measured strain versus temperature curve and  $\alpha_q$  is known,  $1.82\mu\epsilon/\text{ }^\circ\text{C}$  ( $1.01\mu\epsilon/\text{ }^\circ\text{F}$ ). For example, the measured slope of the unidirectional lamina,  $\alpha$ , was  $26.66\mu\epsilon/\text{ }^\circ\text{C}$  ( $14.81\mu\epsilon/\text{ }^\circ\text{F}$ ) in the transverse fiber direction, making  $\alpha_p = 28.48\mu\epsilon/\text{ }^\circ\text{C}$  ( $15.82\mu\epsilon/\text{ }^\circ\text{F}$ ).

The gages used in all of the strain measurements were fully encapsulated "K alloy" with operating temperature ranges from  $-269\text{ }^\circ\text{C}$  to  $+288\text{ }^\circ\text{C}$  ( $-452\text{ }^\circ\text{F}$  to  $+550\text{ }^\circ\text{F}$ ). Two types of gage were used, one having a thermal coefficient of expansion of  $6.0\mu\epsilon/\text{ }^\circ\text{C}$  and the other having a coefficient of  $23.4\mu\epsilon/\text{ }^\circ\text{C}$ . The coefficient of expansion values were chosen to maximize the apparent strain output by taking advantage of thermal mismatches. The apparent strain output is:

$$\epsilon_{\text{app}} = (\alpha_s - \alpha_g) \Delta\phi + \gamma\Delta\phi/S_g.$$

When  $\alpha_s$  is small the output can be increased by making  $\alpha_g$  different from  $\alpha_s$ .

Temperature measurements were made using a bondable resistance temperature sensor. These gages were used in combination with a Linearized Strain Temperature (LST) network which converted the temperature reading to a calibrated strain reading ( $18\mu\epsilon/\text{ }^\circ\text{C}$ ). These gages were bonded to each sample to give a temperature reading of sample surface temperature.

An epoxy based high temperature adhesive with an operating temperature range from -269°C to +371°C (-452°F to +700°F) was used to bond the gages in place. The adhesive was cured at a temperature of 163°C (325°F) for two hours and no post cure was used. All samples were cured at the same temperature and for the same period of time.

At all times during the pretest period the samples were stored in sealed plastic bags containing a dessicant to absorb all entrapped moisture. After the completion of all wet machining and NDT procedure all samples were dried for 24 hours at 121°C (250°F) then again stored in a sealed plastic bag with dessicant.

#### Mechanical Characterization of the Lamina

Tensile tests were conducted at room temperature -54°C (-65°F) and 260°C (500°F) to determine the dependence of mechanical properties on temperature. The tests were conducted in an environmental chamber which has temperature control from -73°C to 260°C (-100°F to 500°F). Air is circulated constantly throughout the test chamber to maintain reasonably uniform temperatures. Cooling was accomplished by liquid nitrogen. Each sample was held at the test temperature for 30 minutes to insure that equilibrium temperature had been reached.

The 0° tensile coupons measured 1.27 cm x 15.24 cm (1/2" x 6") and the 90° coupons measured 2.54 cm x 15.24 cm (1" x 6"). End tabs were manufactured from 3.78 mm (1/8") polyimide circuit board material which was cut into 3.8 cm (1.5") strips and beveled. The end tabs were bonded to the coupons in a special fixture to assure proper alignment. Each coupon was then instrumented with a longitudinal and transverse strain gage (the 06 gage was used).

Chamber temperature was measured by a temperature sensor mounted on a dummy coupon placed in close proximity to the coupon under test. Strain data was taken at known load

increments to generate stress-strain curves. From these curves  $E_A$ ,  $E_T$ ,  $\nu_A$ ,  $\nu_{TA}$  could be determined. Approximately 20 data points were taken from each sample; three samples were tested for each property and test temperature. A linear least squares fit was used to determine the above properties.

#### Thermal Expansion

Thermal coefficients of expansion were measured for unidirectional lamina and  $[\pm 45^\circ]_s$  laminates. Load and relaxation effects upon the coefficient of expansion were also tested on the  $[\pm 45^\circ]_s$  laminate.

The 5 cm x 5 cm (2" x 2") test specimens were suspended in the center of the test section of the environmental chamber for all tests. Both transverse and longitudinal strain gages were mounted on the unidirectional samples, while a single gage was sufficient for the  $[\pm 45^\circ]_s$  laminates. All instrumentation was clustered near the sample center to avoid errors due to edge effects.

For both the unidirectional and  $[\pm 45^\circ]_s$  specimens, the temperature excursion was  $-53^\circ\text{C}$  to  $260^\circ\text{C}$  to  $-53^\circ\text{C}$  ( $-65^\circ\text{F}$  to  $500^\circ\text{F}$  to  $-65^\circ\text{F}$ ). By a complete temperature cycle, hysteresis effects could also be observed. Strain data were recorded at  $-13.9^\circ\text{C}$  ( $25^\circ\text{F}$ ) increments throughout the excursion. A plot of the strain versus temperature for each sample allowed determination of the  $(\varepsilon_p - \varepsilon_q)/\Delta\phi$  slope.

To determine the variation in longitudinal and transverse thermal coefficients with temperature of the unidirectional laminae, the curves were partitioned into temperature intervals and a linear least squares fit applied to data in each interval (the data in the intervals were essentially linear). The coefficients of expansion were determined in each interval by applying equation 3.3. For example, in the  $-53^\circ\text{C}$  to  $38^\circ\text{C}$  ( $-65^\circ\text{F}$  to  $100^\circ\text{F}$ ) temperature range, for sample All,  $(\varepsilon_p - \varepsilon_q)/\Delta\phi$  was  $24.84\mu\varepsilon/\text{ }^\circ\text{C}$  ( $13.80\mu\varepsilon/\text{ }^\circ\text{F}$ ) which yields an  $\alpha_p = 26.66\mu\varepsilon/\text{ }^\circ\text{C}$  ( $14.81\mu\varepsilon/\text{ }^\circ\text{F}$ ). Similarly in that same

temperature range, for sample All,  $(\varepsilon_p - \varepsilon_q)_T / \Delta\phi$  was  $0.70 \mu\text{e}/^\circ\text{C}$  ( $0.39 \mu\text{e}/^\circ\text{F}$ ) in the transverse direction; which makes  $\alpha_T = 1.12 \mu\text{e}/^\circ\text{C}$  ( $0.62 \mu\text{e}/^\circ\text{F}$ ).

The  $[\pm 45^\circ]_5$  test data were collected in the same manner as above. The analysis of the  $[\pm 45]$  data consisted of a linear least squares fit applied to a linear portion of the curve in the  $10^\circ\text{C}$  to  $149^\circ\text{C}$  ( $50^\circ\text{F}$  to  $300^\circ\text{F}$ ) temperature range only.

Compression samples were constructed for the loaded tests. Each sample was made 1.9 cm ( $3/4"$ ) in width with a 1.58 cm ( $5/8"$ ) test section. End tabs were bonded on with a high strength epoxy adhesive and tape was used to prevent bonding in the area adjacent to the test section thus increasing the test section to one inch in length (2.54 cm) but with only  $5/8"$  (1.58 cm) supported. The IITRI compression fixture was used and the constant loading was accomplished by use of a closed loop servo-hydraulic test machine. Tests were run at 150 kg (5.13 ksi or 35.37 MPa), 300 kg (10.26 ksi or 70.74 MPa) and 400 kg (13.33 ksi or 91.77 MPa). Gages were mounted both transversely and longitudinally with respect to the loading direction. Strain was recorded at  $13.9^\circ\text{C}$  ( $25^\circ\text{F}$ ) temperature intervals over the full  $-53^\circ\text{C}$  to  $260^\circ\text{C}$  to  $-53^\circ\text{C}$  ( $-65^\circ\text{F}$  to  $500^\circ\text{F}$  to  $-65^\circ\text{F}$ ) cycle. The results were analyzed in the same manner as the other  $[\pm 45]_5$  results.

Two types of thermal cycles were run to assess relaxation effects. One group of samples was taken from  $260^\circ\text{C}$  to room temperature, stored for 15 days at room temperature, then cooled to  $-53^\circ\text{C}$ . The other samples were taken from  $260^\circ\text{C}$  to room temperature, delayed 15 days and then heated to  $260^\circ\text{C}$ . During the delay period the samples were stored in dessicant except for the 4.5 day period when they were stored in an oven at  $121^\circ\text{C}$ . The first five days of the delay period, samples were stored at room temperature, then the 4.5 day  $121^\circ\text{C}$  treatment was administered followed by a 5.5 day room temperature storage period. Strain data were recorded and analyzed as previously described.

Test Procedure for Thermal Expansion Coefficients  
of Loaded  $[\pm 45]_5$  Laminates

The instrumented sample was placed in the compression fixture which was centered in the environmental chamber. In the no-load condition, the strain gages were zeroed and load was applied to the sample. An initial strain reading was recorded to indicate the no-load strain component and then the chamber temperature was reduced to  $-54^\circ\text{C}$  ( $-65^\circ\text{F}$ ). The sample was heated to  $260^\circ\text{C}$  ( $500^\circ\text{F}$ ) at a rate of approximately  $83^\circ\text{C}/\text{hr}$ . with strain data recorded at  $13.9^\circ\text{C}$  ( $25^\circ\text{F}$ ) temperature intervals. Cooling was initiated immediately at  $260^\circ\text{C}$  ( $500^\circ\text{F}$ ) and strain data were recorded at  $13.9^\circ\text{C}$  ( $25^\circ\text{F}$ ) intervals for the descending temperature excursion to  $-54^\circ\text{C}$  ( $-65^\circ\text{F}$ ). Total test time was approximately seven hours for each test.

Figures 5-8 show plots of longitudinal and transverse strain (plotted is  $\varepsilon_p - \varepsilon_q$ ), which has thus to be adjusted by the quartz thermal expansion) for ascending and descending temperature excursions. All of the plots show hysteresis effects which are most significant in the case of longitudinal expansion. The large increases in compressive longitudinal strain from  $149^\circ\text{C}$  ( $300^\circ\text{F}$ ) to  $260^\circ\text{C}$  ( $500^\circ\text{F}$ ) indicate a considerable loss of stiffness of the laminate in this temperature range, which can probably be due to large creep at those temperatures. The stiffness is regained upon cooling down.

#### 4. RESULTS AND DISCUSSION

Test results have been obtained for the temperature dependent elastic moduli and thermal expansion coefficients for the unidirectional material and for  $\pm 45^\circ$  laminates. The  $\pm 45^\circ$  laminates were selected as a configuration for which comparisons could be made between analytical predictions and experimental results. These laminates were examined to assess the effects of nonlinear stress-strain behavior, time dependent stress-strain behavior, and of externally applied loads upon thermal expansion coefficients of a laminate.

##### Properties of Unidirectional Composites

As shown in table 1, the elastic properties of the unidirectional material are accurately reproducible and their variation with temperature is not very significant. Results for the two thermal expansion coefficients, as shown in table 2, show somewhat erratic behavior, both with respect to variation with temperature and choice of specimen. The scatter is more pronounced for  $\alpha_A$  than for  $\alpha_T$ . The reason for this is that  $\alpha_A$  is a much smaller number, of the order  $2\mu\epsilon^\circ\text{C}$  and the accuracy of thermal expansion coefficient measurements for such small values is questionable. This is an intrinsic problem for all thermal expansion measurements with conventional apparatus.

##### Properties of $\pm 45^\circ$ Laminates

A number of different experiments have been carried out on these  $\pm 45^\circ$  laminates. The major variables examined were the temperature range over which the expansion was measured and the presence or the absence of load during the thermal expansion test. Experimental results are presented in tables 3 and 4. In order to attempt correlation between the theoretical and the experimental results, computation of thermal expansion coefficients has been carried out on the basis of the theory presented earlier utilizing measured

lamina properties. The results for these calculations are shown in table 5. Here calculated average thermal expansions are presented for different starting and finishing temperatures. Calculations of the free thermal expansion coefficient depend upon the Ramberg-Osgood parameter,  $\sigma_y$ , for the transverse stress-strain relation of the unidirectional material. This value is not well known, and hence the computations have been carried out for various assumed yield stress values. Decrease of the value of  $\sigma_y$  implies the increase in nonlinearity. An infinite value of  $\sigma_y$  implies elastic behavior. It is seen that the effect of nonlinearity does not become pronounced unless  $\sigma_y$  has a value below 69 MPa.

#### Free Thermal Expansion

Experimental results for thermal expansion of the  $\pm 45^\circ$  laminate between  $10^\circ$  and  $149^\circ\text{C}$  is shown in table 3a. Comparison of the mean values from the three samples tested with the computed thermal expansion coefficients for the same temperature range as shown in table 5 yield only fair agreement. This comparison between experimental and analytical results is not good enough to assess the importance of nonlinearity for the free expansion coefficients. It should be noted that when the lamina behavior is elastic (whether it be linear or nonlinear) the average thermal expansion coefficients between two temperatures is the same for both heating and cooling over that temperature range. The experimental results indicate a difference between measured thermal expansion on the ascending and descending sections of the measurements.

One underlying difficulty associated with the calculations is the need to assess the temperature at which the laminate is stress free, for expansion coefficient calculations are always performed relative to the stress free state. It is reasonable to assume that a laminate which has been kept for sufficient time at room temperature is stress free since residual stresses will diminish with time by a relaxation

process. When the laminate is heated from this state, internal stresses develop. However, at elevated temperatures such stresses may become very small after a relatively short time since stress relaxation is much more predominant at elevated temperatures.

Table 3b illustrates this effect. Here, during the cool-down from 260°C to room temperature it is reasonable to assume that this high initial temperature was the stress free temperature. The samples were then held for 15 days at room temperature providing an opportunity for stress relaxation. At this point the same temperature range was traversed by heating and, as can be seen in table 3b, the resulting thermal expansion coefficient was significantly higher than during the cooling temperature cycle. Examination of table 5, for the temperature range of room temperature to 260°C, shows that there is reasonable agreement between analysis and experiment for the case in which 260°C is taken as the stress free temperature. Calculations for the heating cycle could not be made because of the uncertainty of material elastic properties at the final high temperature. Such properties are required for the final temperature of the heating experiment as discussed earlier. For this reason subsequent experiments were conducted at lower temperatures.

The effects of delay time were treated at temperatures below room temperature as shown in tables 3c and 3d. Laminate expansion coefficients were measured after cooling from 260°C in the range RT to -54°C. Measurements were made both in the case of a 15 day delay at room temperature and for no delay at room temperature. It is assumed that initially the laminate was stress free at 260°C. When the laminate is cooled without delay to -54°C internal stresses develop and grow with decrease in temperature. In the case of 15 day delay at room temperature it is assumed that the stresses which have formed in cooling from 260°C to room temperature relax to such an extent that they can be neglected. Thus in this case

the laminate is assumed to be stress free at room temperature.

This difference in internal states at room temperature is reflected by the difference in measured thermal expansion coefficients for these two cases. Results of analytical calculations based upon the above assumptions are shown in the lower section of table 5. The same trend is calculated as was observed. For example, for a value of  $\sigma_y$  of 69 MPa, the calculated thermal expansion coefficient is 1.17; while when the delay is assumed to result in a stress free temperature equal to room temperature, the calculated expansion coefficient for the subsequent cooling cycle is equal to 2.27. As can be seen in tables 3c and 3d the respective experimental numbers are 1.17 and 4.74. The expansion coefficients in the RT to  $-54^{\circ}\text{C}$  range increase when there is a long delay at room temperature. However, the measured increase is even larger than the calculated one.

An additional result of interest is the significant difference in thermal expansion coefficients for the cooling and heating parts of the cycle  $\text{RT} \rightarrow -54^{\circ}\text{C} \rightarrow \text{RT}$  as shown in table 3d. This can be explained as follows: it is seen that the internal stress  $\sigma_{22}$  attained at  $-54^{\circ}\text{C}$  is a high tension (table 5,  $\text{RT} \rightarrow -54^{\circ}\text{C}$ , no delay at RT). Thus the thermal expansion coefficient in this range is significantly affected by material nonlinearity. Upon reheating from  $-54^{\circ}\text{C}$  to RT, the transverse stress  $\sigma_{22}$  unloads and it may be considered that the internal strains diminish elastically. Therefore, the thermal expansion coefficient in this heating range is one for an elastic laminate with final elastic properties those of room temperature. For this temperature range that elastic expansion coefficient is 1.51 as compared to the calculated nonlinear value for this temperature range of 1.17 (utilizing  $\sigma_y = 69$  MPa). The experimental result (see table 3d) for heating over this temperature range is larger than for cooling. This agrees qualitatively with the calculated result, but the quantitative difference is much larger than calculated. This suggests the significance of nonlinearities and

time dependence of the material.

### Influence of Applied Loads

The next set of tests is concerned with thermal expansion of a  $\pm 45^\circ$  laminate when subjected to uniaxial compressive loads. Table 6 lists the measured values of the strains in the load direction and perpendicular to the load for various temperatures. In the first part of the table the applied stress was  $\sigma_{11} = 35.4$  MPa, while in the second the applied stress was  $\sigma_{11} = 70.8$  MPa. The shear stress  $\sigma_{12}$  along the fibers in  $\pm 45^\circ$  direction then follows from equation (2.3.5) and the corresponding shear strain  $\epsilon_{12}'$  follows from equation (2.3.12) as:

$$2\epsilon_{12}' = \epsilon_{11} - \epsilon_{22}$$

and is listed in table 6.

Values of the shear modulus at various temperatures have been extracted from the data using the ratios between the constant shear stress and the measured shear strain at that temperature. The loading  $\sigma_{11} = -35.4$  MPa has been used since it can be assumed that for such low loading nonlinearities in shear stress-strain relations are not significant. The shear moduli for the loading  $\sigma_{11} = -70.8$  MPa are smaller than for the lower loading. This can be explained by lamina nonlinearity which becomes more significant at higher loading.

Plots of lamina strains versus temperature for the various loadings are shown in figures 5-8. The behavior is nonlinear and there is a large reduction in material properties at temperatures beyond  $149^\circ\text{C}$ . This accounts for the increases in strain in this temperature range.

Experimental results for the thermal expansion coefficients for the loaded laminate are shown in table 4. It is seen that these expansion coefficients are quite different from the free thermal expansion coefficients of the laminate,

table 3. Furthermore, the expansion coefficients transverse to the load direction are quite different from those in the load direction.

Tables 7-10 summarize computation of thermal expansion coefficients for laminates loaded in compression on the basis of the theory of paragraph 2.3. The results are given for three loadings:  $\sigma_{11}^{\circ} = -35.4, -70.8, -106$  MPa; and for various combinations of "yield stresses" for transverse stress,  $\sigma_y$ , and for shear stress,  $\tau_y$ . For the elastic case ( $\sigma_y = \tau_y = \infty$ ) the expansion coefficients  $\alpha_1^*$  and  $\alpha_2^*$  are the same and equal to the free thermal expansion coefficients of the laminate (see table 5). (Small differences are due to difference in properties at various temperatures considered.)

The calculated results show that nonlinearities have a significant influence on the thermal expansion coefficients. Decrease of  $\sigma_y$  significantly decreases  $\alpha_1^*$  and increases  $\alpha_2^*$ . Decrease of  $\tau_y$  has a similar but much less significant effect. As an example, the results for  $\sigma_y = 69$ , and  $\tau_y = 138$  MPa illustrate the effects of nonlinearity. In the temperature range RT to  $93.3^{\circ}\text{C}$ :  $\alpha_1^* = 1.86$  and  $\alpha_2^* = 3.78$  (in units of  $\mu \text{ cm/cm}/^{\circ}\text{C}$ ); while for an elastic laminate  $\alpha_1^* = \alpha_2^* = 3.01$ . Thus, the theory predicts that the nonlinear loaded laminate is anisotropic in thermal expansion and its thermal expansion coefficients are not equal to the free thermal expansion coefficients. The experimental results show the same effect.

#### Discussion

While the experimental results agree qualitatively with the analytical predictions, the actual numerical agreement cannot be considered satisfactory. There are several possible reasons for the discrepancies.

1. Measured values of thermal expansion coefficients of the unidirectional material have shown considerable scatter, in particular for the longitudinal thermal expansion coefficient  $\alpha_A$ . Lamina thermal expansion

coefficients used in laminate analysis were averages of measured thermal expansion coefficients for several different specimens.

2. The samples supplied for property measurements, both unidirectional and  $\pm 45^\circ$  laminates, were not of high quality. Examination under microscope revealed many defects and flaws.
3. The analysis was based on the assumption that the unidirectional material is nonlinear in response to transverse and shear stresses for loading and unloading. A more realistic approach may be to consider nonlinearity in loading and conventional elastic behavior in unloading. Indeed, one striking effect in thermal expansion behavior (the significant difference in expansion coefficient in the two branches of the thermal cycle  $RT \rightarrow -54^\circ C \rightarrow RT$ ) could be explained by elastic unloading.
4. Thermal expansion analysis presupposes a stress free state at some known reference temperature. In a nonlinear laminate the values of the thermal strains depend on the value of the stress free temperature. However, the stress free temperature is only imperfectly known since it depends on previous history of the laminate. The importance of this phenomenon has been demonstrated here by the differences in free thermal expansion coefficients due to delay times at room temperature when a laminate is cooled from  $260^\circ$  to  $-54^\circ C$ . It may be assumed that a laminate is stress free at its curing temperature. When it is cooled to room temperature significant thermal stresses develop. These stresses relax, thus diminish with time at room temperature. To assess this phenomenon quantitatively a detailed analysis of the time-dependent relaxation of stresses in a laminate

---

is needed. This requires measurement of temperature dependent relaxation moduli and creep compliances of a lamina and their incorporation into laminate analysis. A more fundamental approach would be to measure temperature dependent relaxation moduli and creep compliances for the matrix and then compute such quantities by micromechanics analysis for the unidirectional material (see [3]).

### CONCLUSIONS

The effects demonstrated in this study have serious implications for analysis of laminates which behave nonlinearly in the presence of significant temperature changes. One of the most basic engineering properties of a laminate is its thermal expansion coefficient which determines the thermal strain due to unit temperature rise. When a thermoelastic laminate is heated and loaded the strains due to load and heating are simply superposed. This procedure is still valid when the linear thermoelastic properties of the laminae are temperature dependent. It has been demonstrated in this study, both analytically and experimentally, that this superposition becomes invalid when the mechanical properties of the laminae are nonlinear - that is: the stiffnesses are dependent on the state of stress. In this case the free thermal expansion coefficient is not useful to compute the thermal strains of a laminate due to temperature change in the presence of applied loads. The thermomechanical strains and the internal stresses must be computed by thermomechanical nonlinear laminate analysis.

In summary:

1. Material nonlinearity has a significant effect on the thermal expansion coefficients of laminates.
2. The thermal expansion coefficients for an unloaded and a loaded laminate are significantly different when the laminate deforms in a nonlinear manner. For such a loaded laminate the thermal expansion coefficients are different in direction of load and transverse to load.
3. Experimental data obtained for a symmetric 0/90 laminate indicate that time dependence of the material and the associated stress relaxation significantly affect the values of free thermal expansion coefficients.

#### REFERENCES

1. Chamis, C. C. and Sullivan, T. L., "Analysis of Angle-plied Laminates with Nonlinear Lamination Residual Strains," Presented at ASTM Composite Reliability Conference, Las Vegas, Nevada, April 1974.
2. Hahn, H. T. and Pagano, N. J., "Curing Stresses in Composite Laminates," Journal of Composite Materials, Vol. 9, 1975, pp. 91-106.
3. Hashin, Z., Theory of Fiber Reinforced Materials, NASA CR-1974, 1972.
4. Schapery, R. A., "Deformation and Failure Analysis of Viscoelastic Composite Materials," in Inelastic Behavior of Composite Materials, ASME, AMD - Vol. 13, 1975.
5. McQuillen, E. J., "Viscoelastic Creep and Relaxation in Laminated Composites," Naval Air Development Center Report No. NADC-AM-7115, June 1971.
6. Foye, R. L., "Inelastic Micromechanics of Curing Stresses in Composites," in Inelastic Behavior of Composite Materials, ASME, AMD - Vol. 13, 1975.
7. Hashin, Z., Bagchi, D., and Rosen, B. W., "Nonlinear Behavior of Fiber Composite Materials," NASA CR-2313, 1974.
8. Hahn, H. T. and Tsai, S. W., "Nonlinear Elastic Behavior of Unidirectional Composite Laminae," Journal of Composite Materials, Vol. 7, 1973, pp. 102-118.
9. Foye, R. L., "Theoretical Post-Yielding Behavior of Composite Laminates, Parts I & II - Inelastic Micromechanics," Journal of Composite Materials, Vol. 7, April and July 1973.
10. Petit, P. H. and Waddoups, M. E., "A Method of Predicting the Nonlinear Behavior of Laminated Composites," Journal of Composite Materials, Vol. 3, Jan. 1969, pp. 2-19.
11. Sandhu, R. S., "Nonlinear Response of Unidirectional and Angleply Laminates," AIAA Paper No. 74-380, Presented at the 15th AIAA-ASME Structural Dynamics and Materials Conf., Las Vegas, Nevada, April 1974.

Table 1. Measured Elastic Properties of  
Unidirectional Graphite Polyimide

Material Property	Test Temperature		
	-54°C	RT*	260°C
$E_A$ (MPa)	122.	135.	130.
$E_T$ (MPa)	7.79	8.76	7.10
$v_A$	0.37	0.37	0.30
$v_{TA}$	0.06	0.07	0.02

\*RT was nominally 22°C for these tests.

Table 2. Variation of Thermal Expansion Coefficients with Temperature for Unidirectional G/Pi Laminates

Sample	$\alpha$ $\mu$ in/in	-50	0	50	100	150	200	250	100	50	0	-50	$^{\circ}$ C
A10	$\alpha_A$	-0.41	+	-0.83	+	-0.18	+	-0.76	+	-2.48	+		
A11	$\alpha_A$	-0.14	+	1.44	+	0.11	+	2.39	+	-1.94	+		
A12	$\alpha_A$	1.37	+	-0.11	+	3.19	+	-0.65	+	-2.95	+		
A10	$\alpha_T$	27.6				34.4	+	30.2	+	27.9	+	22.8	+
A11	$\alpha_T$	25.5	+	31.6	+	24.1	+	35.4	+	28.0	+	23.5	+
A12	$\alpha_T$	26.6	+	30.3	+	22.9	+	32.4	+	29.2	+	25.6	+

Table 3. Effect of Temperature and Time Delay on Coefficients of Free Thermal Expansion for  $\pm 45^\circ$  Laminates, ( $\mu\epsilon/^\circ\text{C}$ )

(a) Thermal Expansion without Time Delay

Sample	Ascending $10^\circ - 149^\circ\text{C}$	Descending $149^\circ - 10^\circ\text{C}$
D5	3.87	5.17
C2	5.09	4.75
C3	4.27	5.42
Mean	4.41	5.11

(b) Thermal Expansion with Time Delay

Sample	$260^\circ\text{C} \rightarrow \text{RT}$	Delay Time	$\text{RT} \rightarrow 260^\circ\text{C}$
D4	3.13	15 Days	3.29
C4	3.24	15 Days	5.36
D6	1.80	15 Days	2.52
Mean	2.74	15 Days	3.73

Table 3. Continued

(c) Thermal Expansion with Time Delay

Sample	260°C → RT	Delay Time	RT → -54°C
C5	2.12	15 Days	3.13
D7	1.48	15 Days	6.19
C1	4.32	15 Days	4.91
Mean	1.47	15 Days	4.74

(d) Thermal Expansion without Time Delay

Sample	260°C → RT	Delay Time	RT → -54°C	-54°C → RT
C5	2.12	None	.52	5.06
D7	1.48	None	.70	6.00
C1	4.32	None	2.29	7.16
Mean	2.65	None	1.17	6.34

Table 4. Effect of Loading on Coefficients of Thermal Expansion  
of  $\pm 45^\circ$  G/PI Laminates

Sample	Temp Interval $^\circ\text{C}$	Compressive Stress (MPa)	$^*\alpha_1$ $\mu\text{e}/^\circ\text{C}$	$^*\alpha_2$ $\mu\text{e}/^\circ\text{C}$
D1-1	-51° + 93°	35.4	5.02	9.50
D1-1	-51° + 66°	70.7	9.18	13.23
D1-1	93° + -51°	35.4	4.32	3.51
D1-1	66° + -51°	70.7	3.78	2.32

Table 5. Calculated Thermal Expansion Coefficients of  
G/PI  $\pm 45^\circ$  Laminate (No externally applied loads)

Temperature Range (°C)	Stress Free Temperature	Yield Stress, $\sigma_y$	Ply Stresses			Expansion Coefficient, $\alpha^*$
			$\sigma_{22}$	$\sigma_{11}$	$\sigma_{12}$	
22 - 149	22	$\infty$	28.54	28.54	0	3.15
		138	27.58	27.58		3.07
		69	25.44	25.44		2.90
149 - 10	149	34.5	21.24	21.24		2.55
		$\infty$	28.2	28.2		2.85
		138	27.2	27.2		2.78
260 - 22	260	$\infty$	25.2	25.2		2.63
		138	47.9	47.9		2.85
		69	43.7	43.7		2.68
-54 - 22	22	$\infty$	37.8	37.8		2.42
		138	58.2	58.2		1.51
		69	51.6	51.6		1.32
-54 - 22	22	$\infty$	43.1	43.1		1.17
		138	14.4	14.4		2.34
		69	14.3	14.3		2.32
			13.9	13.9		2.27

Temperature - °C

Stress - MPa

Expansion coefficient -  $10^{-6} \frac{\text{cm}}{\text{cm}} / {}^\circ\text{C} \text{ }^{-1}$

Table 6. Shear Strains on Loaded  $\pm 45^\circ$  Laminate

$\phi$	${}^0\epsilon_{22}$	${}^0\epsilon_{11}$	$\epsilon'_{12}$	$\sigma'_{12}$
${}^0\sigma_{11} = -35.37 \text{ MPa}$				
-51	2.025	-3.185	2.605	-17.72
-18	2.150	-3.050	2.600	-17.72
10	2.285	-2.900	2.539	-17.72
22.2 (RT)	2.395	-2.800	2.598	-17.72
38	2.535	-2.675	2.605	-17.72
66	2.685	-2.525	2.605	-17.72
93	3.150	-2.475	2.813	-17.72
149	3.510	-2.400	2.955	-17.72
204	3.685	-2.700	3.193	-17.72
${}^0\sigma_{11} = 70.74 \text{ MPa}$				
-51	4.550	-6.275	5.413	35.37
-18	4.750	-6.100	5.425	35.57
10	4.975	-5.700	5.338	35.37
22.2 (RT)	5.120	-5.590	5.355	35.37
38	5.300	-5.450	5.375	35.37
66	5.800	-5.450	5.625	35.37
93	6.300	-5.700	6.000	35.37
149	7.050	-6.550	6.800	35.37
204	8.200	-8.300	8.250	35.37

$\phi$  (Temperature) -  ${}^\circ\text{C}$

Stress - MPa

Strain -  $10^{-3} \frac{\text{cm}}{\text{cm}}$

Table 7. Effect of Temperature and Load on Calculated Thermal Expansion Coefficients and Stresses of  $\pm 45^\circ$  G/PI Laminate

$$\sigma_{11} = -35.37 \text{ MPa}$$

Temperature Range	$\sigma_Y$	$\tau_Y$	$\sigma'_{22}$	$\sigma'_{11}$	$\sigma'_{12}$	$\alpha_1^*$	$\alpha_2^*$
RT	93	$\infty$	-15.9	-19.0	17.7	3.01	3.01
	138	69	-16.2	-19.2	1.86	2.71	3.26
	69	34.5	-15.7	-19.7	1.86	1.86	3.95
	34.5	$\infty$	-14.2	-21.2	-0.73	-0.73	6.09
RT	93	138	-16.3	-19.1	17.7	3.00	3.00
	69	69	-16.1	-19.3	2.69	2.69	3.24
	34.5	34.5	-15.6	-19.9	1.86	1.86	3.78
	$\infty$	69	-14.2	-21.2	-0.72	-0.72	6.08
RT	93	138	-16.2	-19.2	17.7	2.98	2.98
	69	69	-16.0	-19.4	2.69	2.69	3.23
	$\infty$	69	-15.5	-19.9	1.87	1.87	3.90

Laminate assumed stress free at RT =  $22^\circ$

$\phi$  (Temperature) -  $^\circ\text{C}$

$\sigma$  (Stress) - MPa

$\alpha^*$  (Expansion Coefficient) -  $\mu \frac{\text{cm}}{\text{cm}} / {}^\circ\text{C}$

Table 8. Thermal Expansion Coefficients and Internal Stresses  
of  $\pm 45^\circ$  Loaded Laminate

$\sigma_{11} = -70.7 \text{ MPa}$						
Temperature Range	$\sigma_y$	$\tau_y$	$\sigma'_{22}$	$\sigma'_{11}$	$\sigma'_{12}$	$\alpha_1^*$
RT	65	$\infty$	-11.7	-59.0	35.3	3.01
	138	$\infty$	-11.6	-59.0	2.53	3.44
	69		-11.4	-59.2	1.18	4.69
	34.5		-10.7	-59.9	-3.37	8.42
RT	65	$\infty$	-11.5	-59.1	35.3	2.97
	138	138	-11.5	-59.2	2.51	3.40
	69		-11.3	-59.4	1.20	4.61
	34.5		-10.6	-60.0	-3.31	8.94

Laminate assumed stress free at RT =  $22^\circ$

Temperature -  $^\circ\text{C}$

Stress - MPa

Expansion Coefficient -  $\nu \frac{\text{cm}}{\text{cm}} / {}^\circ\text{C}$

Table 9. Thermal Expansion Coefficients and Internal Stresses  
of  $\pm 45^\circ$  Loaded Laminate

$$\sigma_{11} = -106 \text{ MPa}$$

Temperature Range	$\sigma_y$	$\tau_y$	$\sigma_{22}$	$\sigma_{11}$	$\sigma_{12}$	$\alpha_1^*$	$\alpha_2^*$
RT	$\infty$	$\infty$	-19.1	-87.2	53.2	3.01	3.01
	138		-18.8	-87.5		1.88	3.75
	69		-18.0	-88.3		-1.08	6.62
	34.5		-16.0	-90.3		-9.70	15.00
RT	$\infty$	138	-18.9	-87.8	53.2	2.93	2.93
	138		-18.2	-88.1		1.88	3.90
	69		-17.5	-88.8		-0.93	6.52

Laminate assumed stress free at RT =  $22^\circ$

Temperature -  $^\circ\text{C}$

Stress - MPa

Expansion Coefficient -  $\mu \frac{\text{cm}}{\text{cm}}/\text{ }^\circ\text{C}$

Table 10. Thermal Expansion Coefficients and Internal Stresses  
of  $\pm 45^\circ$  Loaded Laminate

$$^0\sigma_{11} = -35.4 \text{ MPa}$$

Temperature Range	$\sigma_y$	$\tau_y$	$\sigma'_{22}$	$\sigma'_{11}$	$\sigma'_{12}$	$\alpha_1^*$	$\alpha_2^*$
149	93	$\infty$	10.6	-46.1	17.7	3.01	3.01
	138		10.6	-46.0		3.46	2.36
	69		10.4	-45.9		4.55	0.83
	34.5		9.9	-45.3		7.29	-2.78
149	93	$\infty$	10.6	-46.1	17.7	2.99	2.99
	138		10.6	-46.0		3.44	2.34
	69		10.4	-45.9		4.52	0.84
	34.5		9.9	-45.3		7.23	-2.74

Laminate assumed stress free at  $149^\circ\text{C}$

Temperature -  $^\circ\text{C}$

Stress - MPa

Expansion Coefficient -  $\mu \frac{\text{cm}}{\text{cm}}/\text{ }^\circ\text{C}$

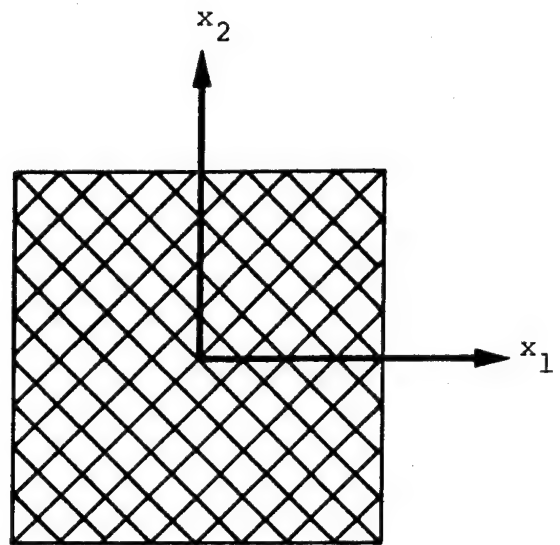


Figure 1. Laminate Coordinate System

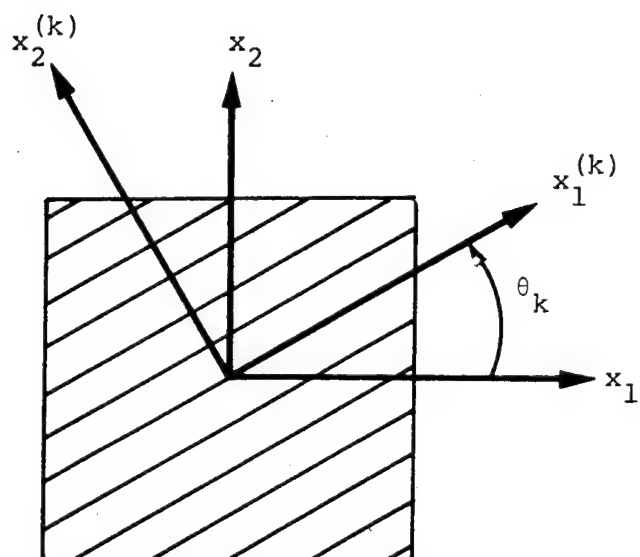


Figure 2. Laminate Coordinate System

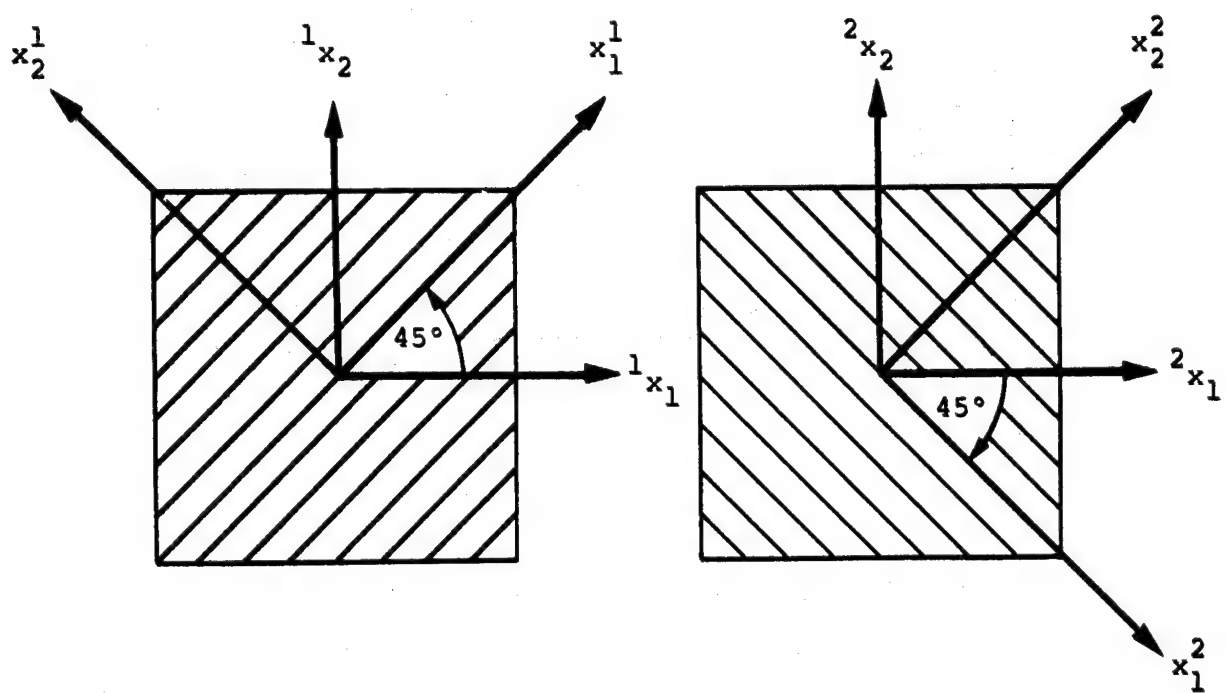
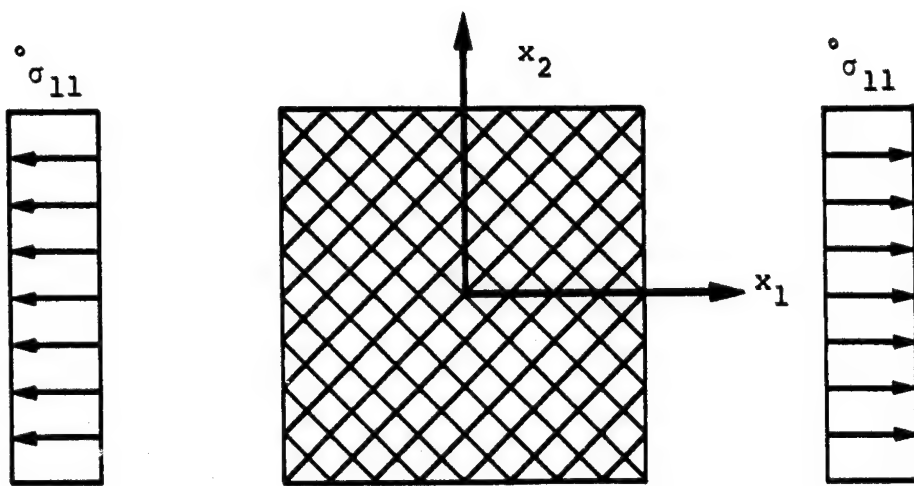
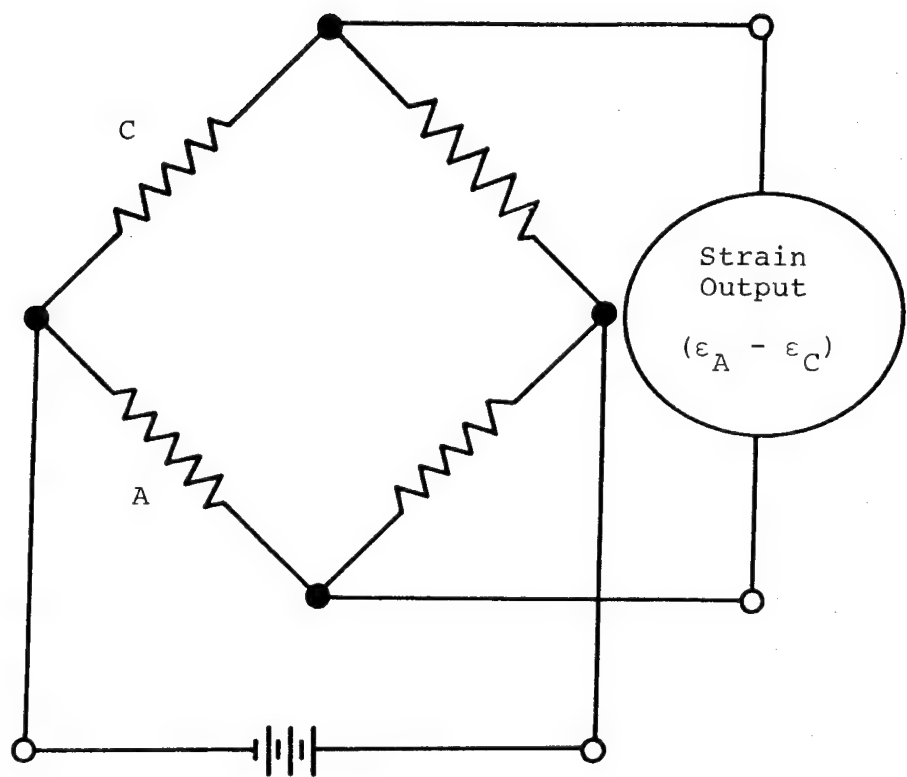


Figure 3.  $\pm 45^\circ$  Laminate



A = Active gage mounted on polyimide

C = Compensation gage mounted on quartz

Figure 4. Half Bridge Circuit Used in Temperature Compensated Tests

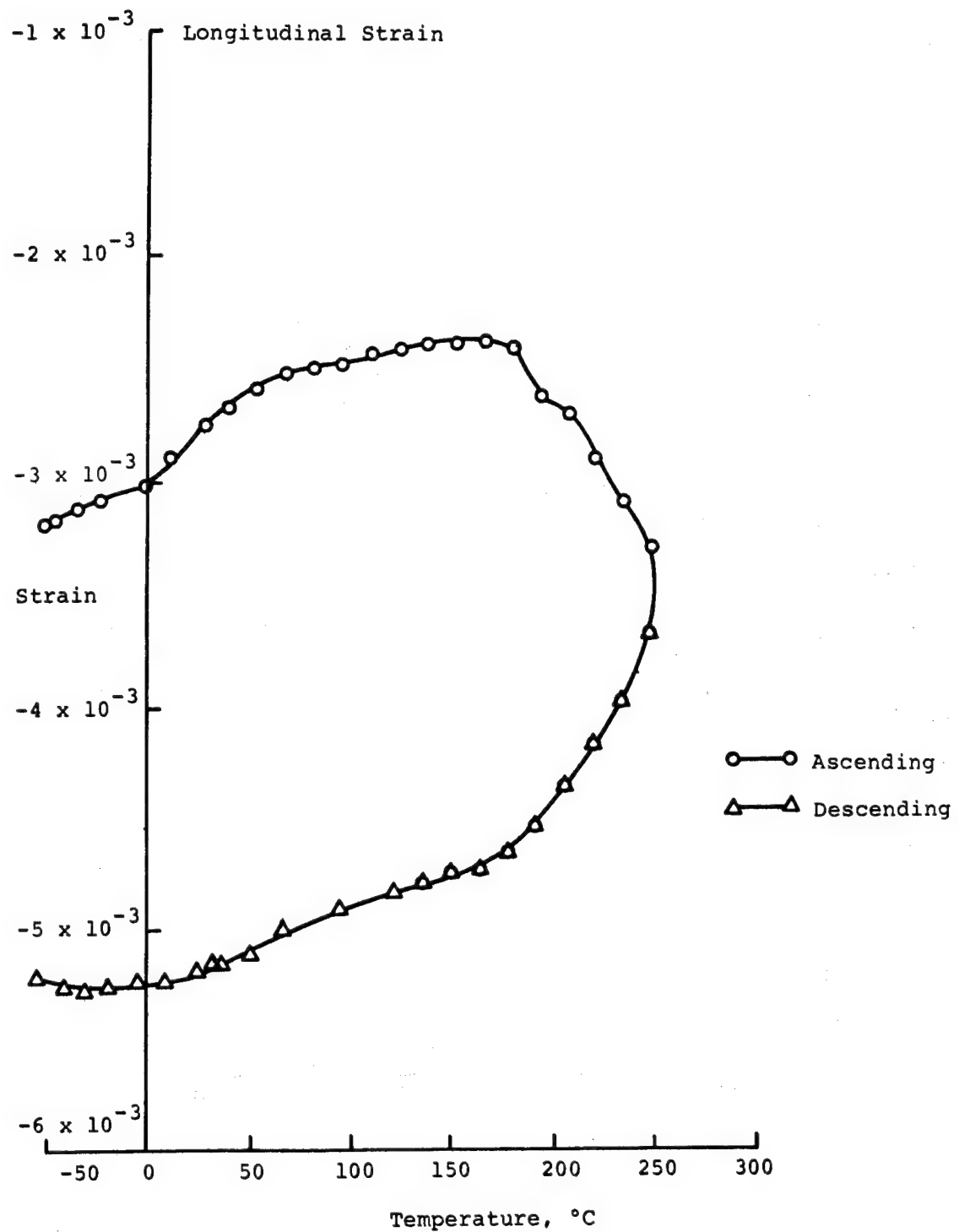


Figure 5. Longitudinal Strain ( $\epsilon_p - \epsilon_q$ ) versus Temperature Load  
 $\sigma_{11} = -1473 \text{ N} \text{ (-150 kg)}$        $\sigma_{11} = -35.37 \text{ MPa}$

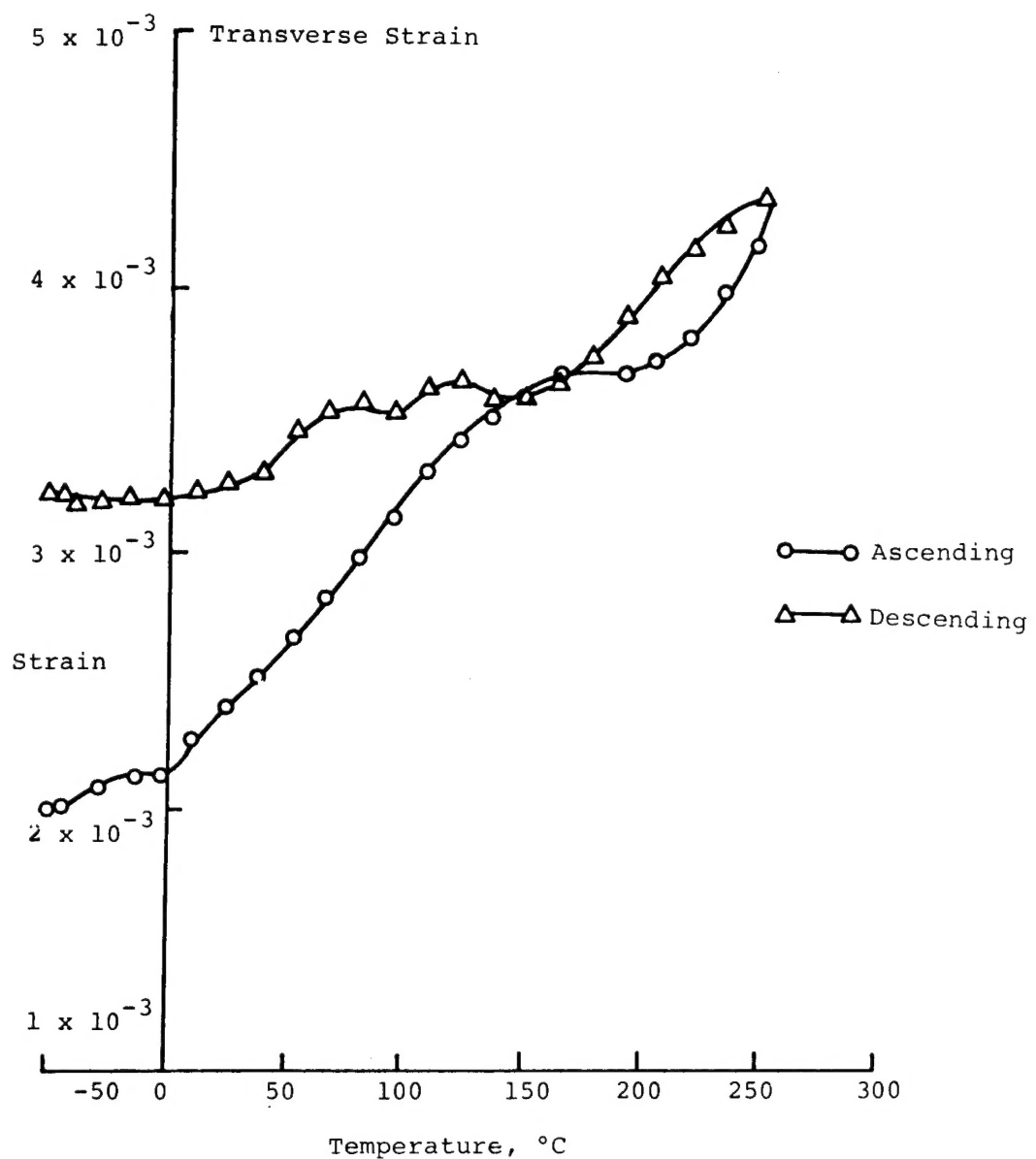


Figure 6. Transverse Strain versus Temperature Load  
 $= -1473 \text{ N } (-150 \text{ kg}) \quad \sigma_{11} = -35.37 \text{ MPa}$

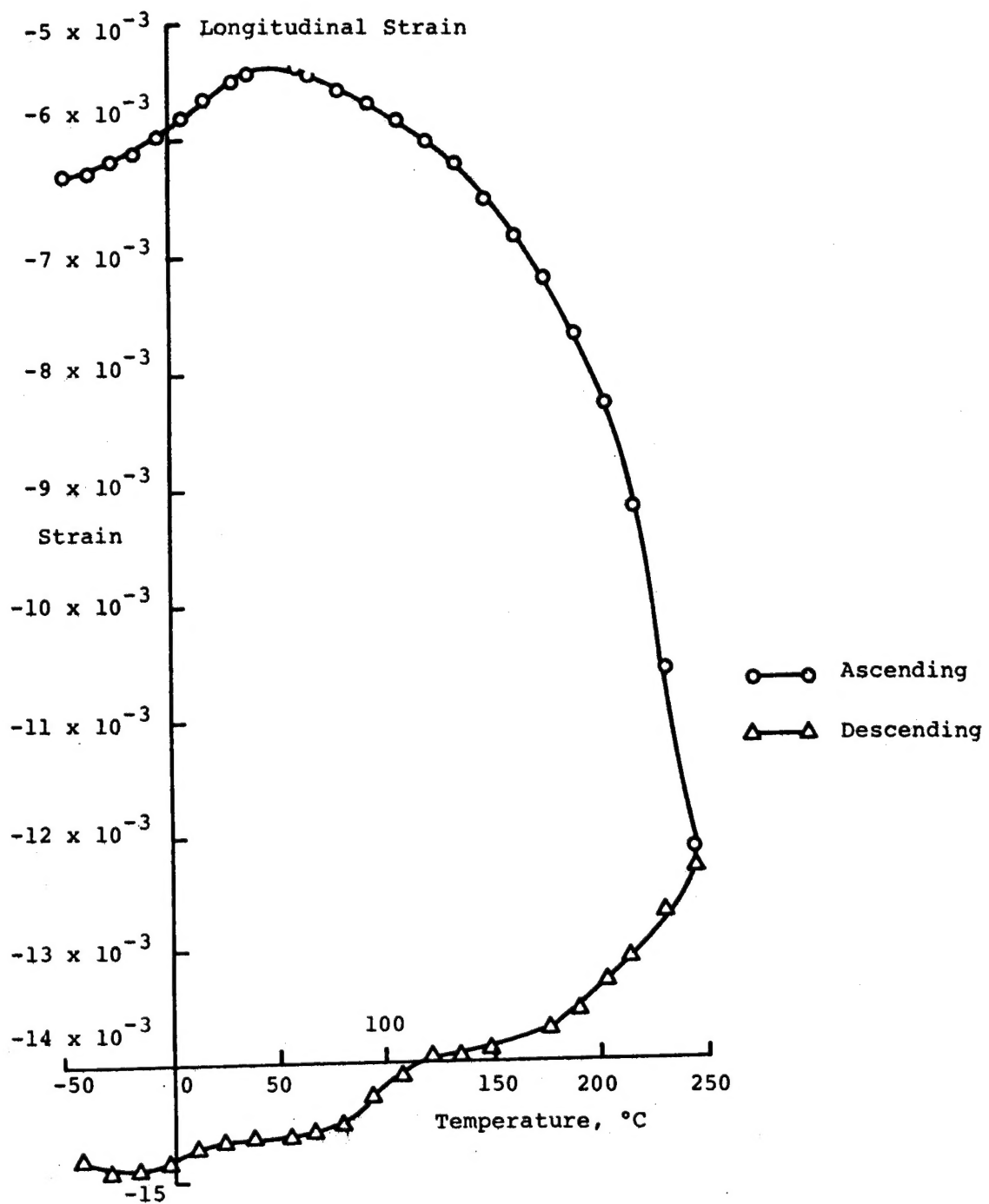


Figure 7. Longitudinal Strain versus Temperature Load  
 $= -2946 \text{ N} (-300 \text{ kg}) \quad \sigma_{11} = -70.74 \text{ MPa}$

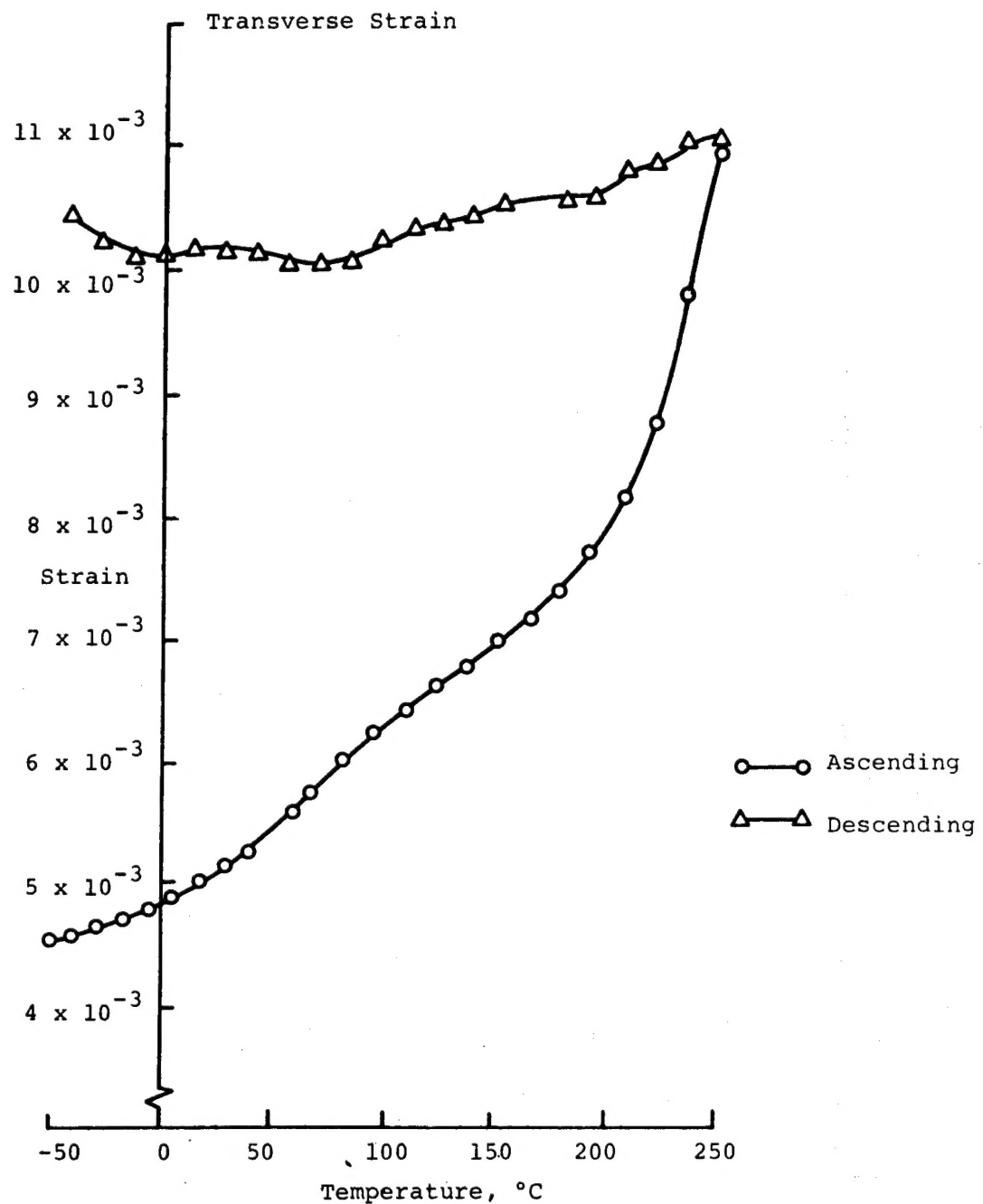


Figure 8. Transverse Strain versus Temperature Load  
 $= -2946 \text{ N } (-300 \text{ kg}) \quad \sigma_{11} = -70.74 \text{ MPa}$

1. Report No. NASA CR-3088	2. Government Accession No.	3. Recipient's Catalog No.	
4. Title and Subtitle NONLINEAR EFFECTS ON COMPOSITE LAMINATE THERMAL EXPANSION		5. Report Date February 1979	
		6. Performing Organization Code	
7. Author(s) Z. Hashin, B.W. Rosen, and R. B. Pipes		8. Performing Organization Report No. MSC/TFR/800/1015	
9. Performing Organization Name and Address Material Sciences Corporation Blue Bell, PA 19422		10. Work Unit No. 524-71-01-01	
12. Sponsoring Agency Name and Address National Aeronautics and Space Administration Washington, D.C. 20546		11. Contract or Grant No. NAS1-14964	
		13. Type of Report and Period Covered Contractor Report	
		14. Sponsoring Agency Code	
15. Supplementary Notes Langley Technical Monitor: Howard M. Adelman Final Report			
16. Abstract <p>The thermomechanical behavior of unidirectionally fiber reinforced laminae in plane stress has been described by a set of nonlinear thermomechanical stress-strain relations. A general procedure for analysis of in-plane loaded symmetric laminates, composed of such laminae, has been established for simultaneous loading and temperature inputs. A <math>\pm 45^\circ</math> laminate subjected to heating and uniaxial load has been analyzed in detail.</p> <p>Analyses of Graphite/Polyimide laminates have shown that the thermomechanical strains cannot be separated into mechanical strain and free thermal expansion strain. Consequently the free thermal expansion coefficient is generally not useful for computation of thermal strains in a loaded nonlinear laminate. Moreover, a laminate such as the <math>\pm 45^\circ</math> which behaves isotropically for free thermal expansion behaves anisotropically when loaded and heated.</p> <p>Elastic properties and thermal expansion coefficients of unidirectional Graphite/Polyimide specimens were measured as a function of temperature to provide inputs for the analysis. The <math>\pm 45^\circ</math> symmetric Graphite/Polyimide laminates were tested to obtain free thermal expansion coefficients and thermal expansion coefficients under various uniaxial loads.</p> <p>The experimental results demonstrated the effects predicted by the analysis, namely dependence of thermal expansion coefficients on load, and anisotropy of thermal expansion under load. Numerical agreement of analytical and experimental results was fair. The significance of time dependence on thermal expansion was demonstrated by comparison of measured laminate free expansion coefficients with and without 15-day delay at intermediate temperature.</p>			
17. Key Words (Suggested by Author(s)) composite materials thermal expansion thermal stress nonlinear behavior		18. Distribution Statement Unclassified - Unlimited Subject Category 39	
19. Security Classif. (of this report) Unclassified	20. Security Classif. (of this page) Unclassified	21. No. of Pages 56	22. Price* \$5.25